Competition between superconductivity and magnetic/nematic order as a source of anisotropic superconducting gap in underdoped $Ba_{1-x}K_xFe_2As_2$

H. Kim,[1] M. A. Tanatar,[1,2] W. E. Straszheim,[1] K. Cho,[1] J. Murphy,[2] N. Spyrison,[2] J.-Ph. Reid,[3] Bing Shen,[4] Hai-Hu Wen,[4] R. M. Fernandes,[5] and R. Prozorov[1,2,*]

[1]*Ames Laboratory, Ames, Iowa 50011, USA*

[2]*Department of Physics & Astronomy, Iowa State University, Iowa 50011, USA*

[3]*Departement de Physique & RQMP, Universite de Sherbrooke, Sherbrooke, Canada*

[4]*Center for Superconducting Physics and Materials, National Laboratory of Solid State Microstructures & Department of Physics, Nanjing University, Nanjing 210093, China*

[5]*School of Physics and Astronomy, University of Minnesota, Minneapolis, Minnesota 55455, USA*

(Received 9 June 2014; revised manuscript received 1 July 2014; published 28 July 2014)

The in-plane London penetration depth $\Delta\lambda(T)$ was measured using a tunnel diode resonator technique in single crystals of $Ba_{1-x}K_xFe_2As_2$ with doping levels x ranging from heavily underdoped, $x = 0.16$ ($T_c = 7$ K), to nearly optimally doped, $x = 0.34$ ($T_c = 39$ K). Exponential saturation of $\Delta\lambda(T)$ in the $T \to 0$ limit is found in optimally doped samples, with the superfluid density $\rho_s(T) \equiv [\lambda(0)/\lambda(T)]^2$ quantitatively described by a self-consistent γ model with two nodeless isotropic superconducting gaps. As the doping level is decreased towards the extreme end of the superconducting dome at $x = 0.16$, the low-temperature behavior of $\Delta\lambda(T)$ becomes nonexponential and is best described by the power law $\Delta\lambda(T) \propto T^2$, characteristic of strongly anisotropic gaps. The change between the two regimes happens within the range of coexisting magnetic/nematic order and superconductivity, $x < 0.25$, and is accompanied by a rapid rise in the absolute value of $\Delta\lambda(T)$ with underdoping. This effect, characteristic of the competition between superconductivity and other ordered states, is very similar to but of significantly smaller magnitude than what is observed in the electron-doped $Ba(Fe_{1-x}Co_x)_2As_2$ compounds. Our study suggests that the competition between superconductivity and magnetic/nematic order in hole-doped compounds is weaker than in electron-doped compounds, and that the anisotropy of the superconducting state in the underdoped iron pnictides is a consequence of the anisotropic changes in the pairing interaction and in the gap function promoted by both magnetic and nematic long-range orders.

DOI: 10.1103/PhysRevB.90.014517 PACS number(s): 74.70.Xa, 74.20.Rp, 74.62.Dh

I. INTRODUCTION

The experimental determination of the symmetry of the superconducting gap is important to unravel the mechanism of superconductivity in iron-based superconductors [1–3]. Measurements of the London penetration depth [4–6], thermal conductivity [7,8], and specific heat [9–11] in electron doped $Ba(Fe_{1-x}Co_x)_2As_2$ (BaCo122) suggest that the superconducting gap changes significantly with doping, developing nodes at both overdoped and underdoped dome edges [8,12,13]. This doping evolution is very similar to what is observed in another electron-doped family, $NaFe_{1-x}Co_xAs$ [14,15] and LiFeAs [16–19]. It is also consistent with the predicted dependence of the gap function with doping in the s^{+-} model [13,20,21]. On the other hand, nodal behavior is observed at all doping levels in isovalent-substituted $BaFe_2(As_{1-x}P_x)_2$ (BaP122) [22]. This remarkable contrast in two systems that share the same parent compound prompts a detailed study of the hole doped $Ba_{1-x}K_xFe_2As_2$ (BaK122) materials.

In BaK122, a full isotropic gap has been reported in compositions close to optimal [23–29], whereas strongly overdoped compositions with $x \approx 1$ display nodal superconductivity [29–34]. Although these observations suggest a similar trend as compared to the electron-doped BaCo122 materials [35], there has been no systematic studies of the superconducting gap structure in the underdoped BaK122 so far. In this doping regime, superconductivity microscopically coexists and competes with long-range magnetic/nematic order [20,32,36], making this an ideal system to investigate the rich interplay between these ordered states [37,38]. Interestingly, a sizable asymmetry between the normal state properties of the electron- and hole-doped materials is observed in such underdoped regime [39–41].

In this work, we study the evolution of the temperature dependence of the in-plane London penetration depth, $\Delta\lambda(T)$, in high-quality single crystals of $Ba_{1-x}K_xFe_2As_2$ across the underdoped region of the phase diagram, $0.16 \leqslant x \leqslant 0.34$. We find that the optimally doped samples show a weak exponential temperature dependence in the $T \to 0$ limit, suggesting nodeless isotropic gaps. This conclusion is consistent with the temperature dependence of the superfluid density, which can be well fitted using the self-consistent γ model with two full gaps in the clean limit [42]. In contrast, the lowest-T_c samples, deep in the underdoped regime, show a strong power-law temperature dependence of $\Delta\lambda(T)$ in the low-T limit, typical of strongly anisotropic gaps. The onset of this behavior roughly correlates with the onset of magnetic/nematic transition. This may indicate that the anisotropic changes in the pairing interaction arising from the coexistence of superconductivity and nematicity play a major role in determining the gap structure in the underdoped regime. The magnitude of $\Delta\lambda(0.25T_c)$, which serves as a proxy of the magnitude of the zero-temperature penetration depth, shows a rapid rise in the range of coexisting magnetic/nematic order

*Corresponding author: prozorov@ameslab.gov

and superconductivity. Comparison with the penetration depth data in the electron-doped counterpart $Ba(Fe_{1-x}Co_x)_2As_2$ reveals that the rapid rise of $\Delta\lambda$ in the coexistence state is similar in both materials, as expected for competing electronic ordered states [43–46]. However, the increase in $\Delta\lambda$ is almost three times larger in electron-doped materials, suggesting that the competition between magnetic/nematic order and superconductivity is weaker in the hole-doped materials. Interestingly, this electron-hole asymmetry inside the superconducting state correlates with the asymmetric behavior of the normal state properties, in particular, the nematic susceptibility, as measured by the in-plane resistivity anisotropy [39] and by elastic constant measurements [47], and pseudogap features in the interplane resistivity [48,49].

II. EXPERIMENTAL

The growth and characterization of single crystals of BaK122 used in this study is described in detail in previous reports [49,50]. In brief, measurements were performed on pre-screened crystals with sharp superconducting transitions and individually measured chemical compositions with wavelength dispersive x-ray spectroscopy (WDS) in *JEOL JXA-8200* electron microprobe. The composition was measured for 12 points per single crystal and averaged, yielding statistical errors of compositional measurement of ± 0.005. The London penetration depth $\Delta\lambda(T)$ was measured using the tunnel-diode resonator technique [51–53] in our He^3 and dilution refrigerator setups; details of the calibration procedure and data analysis can be found in Ref. [54].

III. RESULTS AND DISCUSSION

In Fig. 1(a), we show the variation of the London penetration depth $\Delta\lambda(T)$ from the base temperature to T_c for five compositions of $Ba_{1-x}K_xFe_2As_2$ spanning from $x = 0.16$ ($T_c = 7$ K, edge of the superconducting dome) to $x = 0.34$ ($T_c = 39$ K, nearly optimally doped). The data are normalized by $\Delta\lambda(T_c)$ and reveal the high quality of our single crystals as evidenced by the sharpness of the superconducting transitions and the absence of any additional features. In Fig. 1(b), we present the same data plotting the actual $\Delta\lambda(T)$ as function of the reduced temperature T/T_c for $0 < T/T_c \leqslant 0.3$. This is the characteristic temperature range in which the superconducting gap of single-band superconductors can be considered constant, and in which the temperature dependence of $\Delta\lambda(T)$ reflects the nodal structure of the gap. In the clean limit, $\Delta\lambda(T)$ is expected to depend exponentially on temperature in isotropic nodeless superconductors, whereas a linear-in-T behavior is expected for superconductors with line nodes. Because the experimental verification of the exponential dependence is difficult due to noise in the data, the standard procedure is to fit the data to a power-law function, $\Delta\lambda(T) = AT^n$. In this case, exponents $n \gtrsim 3$ usually indicate nodeless gap, whereas $n \lesssim 2$ indicate strong gap anisotropies—either due to nodes in the presence of impurity scattering or due to very deep gap minima [14]. In Fig. 1(b), the data are plotted as a function of $(T/T_c)^2$. Several features can be noticed; first, the samples at the very edge of the dome, $x = 0.16$, display a temperature dependence very close to T^2, signaling a sizable gap anisotropy. As optimal doping is approached, the magnitude of $\Delta\lambda(0.3T_c)$ dramatically decreases and the $\Delta\lambda(T)$ curves progressively flatten at low temperatures. This flattening signals a full-gap state, though we note that data for $T/T_c > 0.15$ approximately follow a T^2 behavior.

To shed light on the behavior at optimal doping, in Fig. 2, we show the superfluid density, $\rho_s(T) = \lambda^2(0)/\lambda^2(T)$ of the $x = 0.34$ sample. Here, $\lambda(T) = \Delta\lambda(T) + \lambda(0)$ is obtained by using $\lambda(0) = 200$ nm [55] as the value of the London

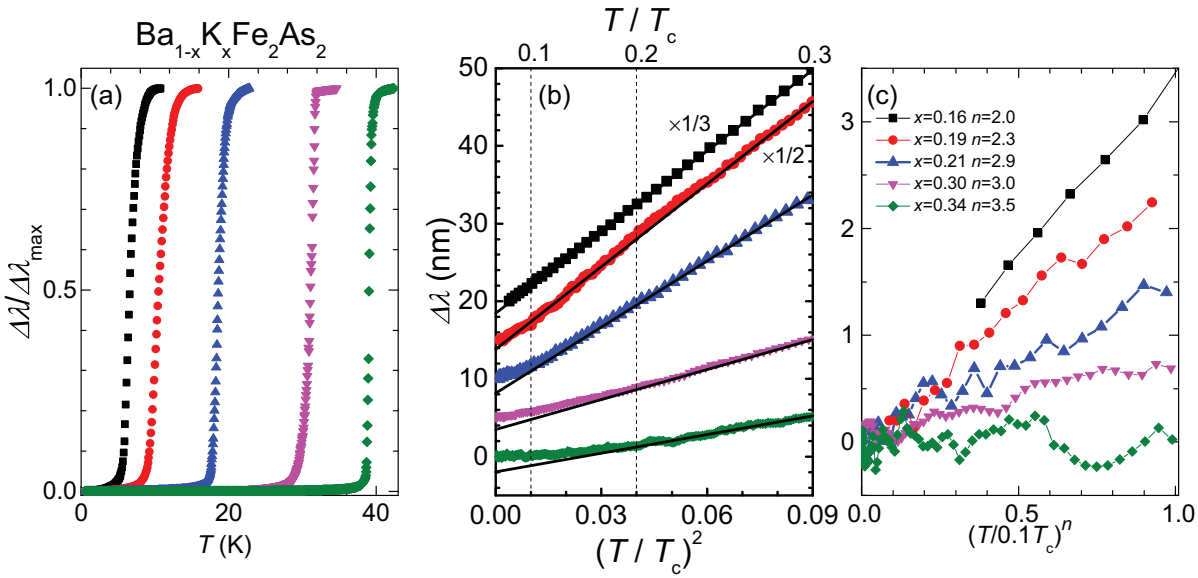

FIG. 1. (Color online) (a) Normalized $\Delta\lambda(T)$ for samples of $Ba_{1-x}K_xFe_2As_2$ with $x = 0.16$, 0.19, 0.21, 0.3, and 0.34 (left to right). (b) Zoom of the actual $\Delta\lambda(T)$ plotted vs $(T/T_c)^2$ for a range $T/T_c \leqslant 0.3$. The *actual* data for $x = 0.16$ were divided by a factor of 3 ($\times 1/3$) and for $x = 0.19$ were divided by a factor of 2 ($\times 1/2$), respectively, to facilitate the comparison with other compositions; (c) shows the same data over the lowest temperature range $T/T_c \leqslant 0.1$, plotted as a function of $(T/0.1T_c)^n$ with n 2.0, 2.3, 2.9, 3.0, and 3.5 ± 0.1 for $x = 0.16$, 0.19, 0.21, 0.3, and 0.34, respectively. Note the systematic decrease of $\Delta\lambda(T)$ on approaching optimal doping.

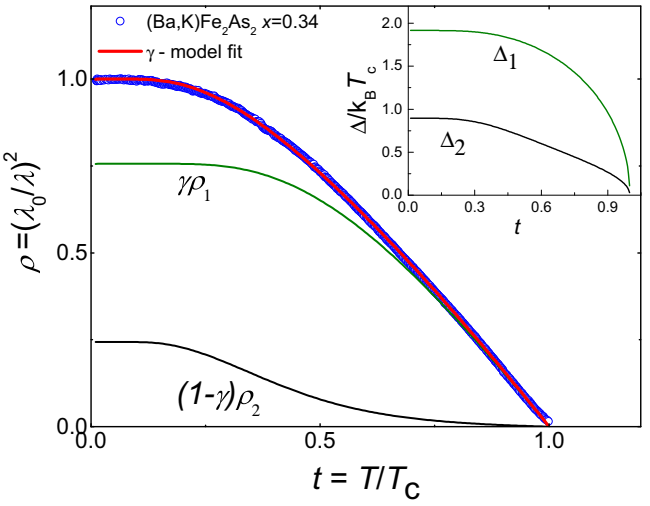

FIG. 2. (Color online) Superfluid density, $\rho_s(T) \equiv [\lambda(0)/\lambda(T)]^2$, of the optimally doped sample $Ba_{1-x}K_xFe_2As_2$, $x = 0.34$, calculated from the data of Fig. 1 using $\lambda(0) = 200$ nm [55] (open symbols). The solid red line on top of the data is the fit using the self-consistent two-gap γ model, with the black and green curves in the main panel denoting the partial superfluid densities ρ_1 (larger gap) and ρ_2 (smaller gap). The temperature dependence of the corresponding gaps Δ_1 and Δ_2 is shown in the inset.

penetration depth in the $T \to 0$ limit. The superfluid density $\rho_s(T)$ shows a clear saturation at low temperatures, evidencing a full-gap superconducting state, similar to the data of Fig. 1(b). A more detailed analysis of the $\rho_s(T)$ data was made using the clean-limit γ model to fit the data [42], as shown by the red solid line in the same figure. Here, $\rho_s = \gamma\rho_1 + (1-\gamma)\rho_2$; the partial superfluid densities ρ_1 and ρ_2 are shown in the main panel of Fig. 2, whereas the superconducting gaps $\Delta_1(T)$ and $\Delta_2(T)$ are shown in the inset of Fig. 2. The estimated gap values in the $T \to 0$ limit are 6.5 and 3.3 meV, the larger gap being in reasonable agreement with the value of ~6 meV found from specific heat measurements [56]. This analysis implies that the small superconducting gap, Δ_2, is strongly temperature dependent even for $T < 0.3T_c$, and the characteristic behavior can be found only at temperatures at least two times lower than $0.3T_c$. In Fig. 1(c), we show the data over the temperature range $0 < T/T_c \leqslant 0.1$, presented as a power-law function T^n of the reduced temperature, with exponent n as shown in the main panel.

In Fig. 3, we summarize the doping evolution of the London penetration depth as found in our study. For reference in the top panel Fig. 3(a), we show the doping phase diagram as determined from our TDR and resistivity measurements [49], which are in good agreement with the phase diagram determined from neutron scattering and magnetization data on polycrystalline samples by Avci *et al.* [57]. This analysis reveals two clear trends. (i) The exponent n of the power-law temperature dependence of $\Delta\lambda$, Fig. 3(b), as determined from the data analysis for $0 < T \leqslant T_{up}$ with $T_{up} = 0.1T_c$ and $0.15T_c$, decreases from $n = 3.5$ for $x = 0.34$ (which is technically indistinguishable from an exponential dependence) to $n = 2$ for $x = 0.16$. (ii) The actual variation of the London penetration depth $\Delta\lambda(T_{up})$ with $T_{up} = 0.3T_c$ and $0.15T_c$—which mimics the doping dependence

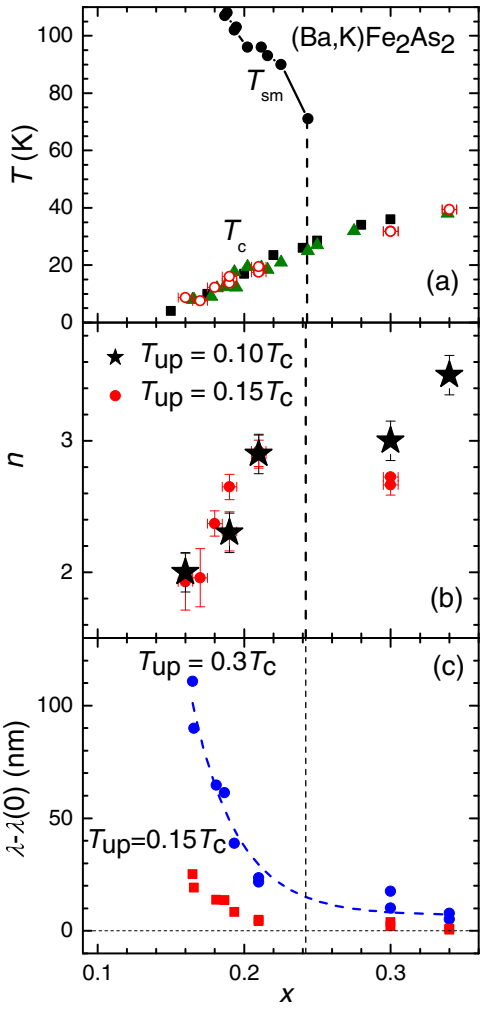

FIG. 3. (Color online) (a) Doping phase diagram of $Ba_{1-x}K_xFe_2As_2$ as determined from resistivity and TDR measurements on single crystals [49] (black circles show T_{sm} and black squares show T_c), matching well the results on polycrystalline samples [57,58] (green triangles). Open red circles represent the samples used in the present study of the penetration depth. Dashed line shows an extrapolation of the orthorhombic/magnetic transition line, $T_{sm}(x)$ to $T \to 0$. Panel (b) shows the doping evolution of the exponent of the power-law function n as determined from the data analysis in the temperature range $T/T_c \leqslant 0.1$ (black stars) and $T/T_c \leqslant 0.15$ (red circles). Panel (c) shows the doping evolution of the magnitude of the variation of the London penetration depth at low temperatures, $\Delta\lambda(T_{up})$ with $T_{up} = 0.15T_c$ (red squares) and $T_{up} = 0.3T_c$ (blue circles).

of the zero-temperature penetration depth—strongly increases in the same doping regime.

Both effects are more prominent for doping levels $x \leqslant 0.21$, where magnetism and nematicity are also present. Indeed, these trends can be understood theoretically as a result of the competition and coexistence between magnetic/nematic order and superconductivity [59]. On the one hand, magnetism competes with superconductivity for the same electronic states [20,36], which is most directly revealed by the suppression of the magnetic order parameter below T_c seen in neutron scattering [57]. Due to its magnetic origin,

nematic order inherits this competition and also competes with superconductivity [60,61], as manifested by the decrease of the orthorhombic distortion—proportional to the nematic order parameter [38]—below T_c, as measured by x-ray scattering [57]. The competition between these electronic ordered states results in a suppression of the zero-temperature superfluid density, and a consequent enhancement of the penetration depth in the low-temperature limit [43–46], in qualitative agreement with the experimental data.

On the other hand, coexistence with magnetic/nematic order leads to strong anisotropies in the gap function, which is also in qualitative agreement with the experimental data. Consider for instance a simplified scenario in which the s^{+-} gap function and the pairing interaction are completely isotropic at optimal doping. Because nematic order breaks the tetragonal symmetry of the system, it gives rise to a d-wave component in the original s^{+-} gap function in the coexistence state [62,63]. Due to the proximity between the d-wave and s^{+-} ground-state energies [64]—as manifested by the existence of a Bardasis-Schrieffer mode in the Raman spectrum of the optimally doped samples [65]—this mixing between d-wave and s^{+-} states can be sizable, leading to strong anisotropies in the gap. Furthermore, long-range magnetic order promotes anisotropy in the pairing interaction itself [37]. Due to the anisotropic reconstruction of the Fermi surface caused by the doubling of the unit cell in the magnetic phase, the electronic states near the Fermi level acquire a significant angular dependence, which is translated to an effectively anisotropic pairing interaction for the states of the reconstructed Fermi surface. As a result, the gaps, that were fully isotropic in the noncoexistence state, develop deep minima, which may even give rise to the nodal behavior [37].

It is instructive to compare our observations in the hole-doped BaK122 with the behavior of electron-doped BaCo122. Figure 4 compares the doping phase diagrams [panel (a)] and doping evolutions of the London penetration depth [panel (b)] of the hole- and electron-doped $BaFe_2As_2$ with K and Co, respectively. The magnetic, T_m, structural, T_s, and superconducting, T_c, transitions in single crystals of BaCo122 were determined by the neutron scattering and magnetization measurements in Ref. [36]. They found that the structural transition line terminates at $x_s = 0.063$. In BaCo122 $T_m(x)$ line is below $T_s(x)$ for all doped compositions. Similar measurements in polycrystalline hole-doped BaK122 were performed by Avci *et al.* [57], where they determined $x_s = 0.25$. The T_s and T_m lines coincide for all doping levels. The results for BaK122 were later reproduced on single crystals, which we used for this study [49]. The penetration depth data for BaCo122 were taken from Ref. [4].

In order to directly compare hole- and electron-doped compounds, we normalize the x axis by the critical values x_s. This comparison reveals very interesting similarities and differences between these two types of doping. First, as can be seen from Fig. 4, the $T_s(x)$ boundary in BaK122 terminates very sharply, suggesting a possible first-order transition with doping between the orthorhombic/nematic and tetragonal phases. Second, the rapid increase of the London penetration depth $\Delta\lambda(T_{up})$ with underdoping, reflecting the increase of $\lambda(0)$ [59], has very different magnitudes for the two types of doping. For instance, despite using BaK122 samples

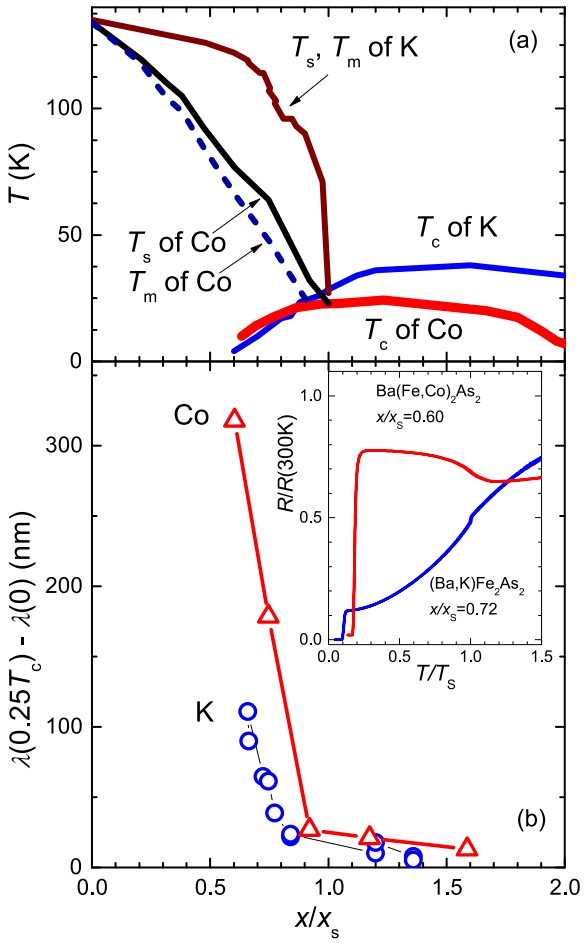

FIG. 4. (Color online) (a) Comparison of the doping phase diagrams of hole-doped $Ba_{1-x}K_xFe_2As_2$ and of the electron-doped $Ba(Fe_{1-x}Co_x)_2As_2$. The data are plotted using normalized x/x_s composition scale, where x_s is a doping boundary of $T_s(x)$ lines with $x_s = 0.25$ for BaK122 [57] and $x_s = 0.063$ for BaCo122 [36], respectively. (b) Doping evolution of the temperature-dependent part of London penetration depth $\Delta\lambda(0.25T_c)$ in K-doped (blue circles) and Co-doped (red triangles) samples. Note the three times difference in the magnitude of penetration depth increase in two cases. Inset in (b) shows normalized temperature-dependent resistivity, $R/R(300K)$, for underdoped samples with Co-doping $x = 0.038$, $x/x_s = 0.6$ and K-doping $x = 0.18$, $x/x_s = 0.72$, plotted using normalized temperature scale, T/T_s. Note that the resistivity of K-doped samples shows very small change at T_s, while that of Co-doped samples increases significantly below T_s.

that are much closer to the edge of the superconducting dome ($T_c = 7$ K for $x = 0.16$) than in our previous study of BaCo122 compounds ($T_c = 7.4$ K for $x = 0.038$) [59], we find a three times smaller increase of $\Delta\lambda(0.25T_c)$ on the hole-doped side compared to the electron-doped side. This suggests weaker competition between magnetic/nematic order and superconductivity in the hole-doped BaK122 than in the electron-doped BaCo122, which is in line with the significantly weaker suppression of the magnetic order parameter below T_c found in neutron scattering experiments [36,57] and nuclear magnetic resonance measurements [32]. Similarly, as shown in the inset of panel (b) in Fig. 4, the feature in the temperature dependent normalized resistivity in the normal state is much

clearer in BaCo122, than in BaK122. This suggests that the part of the Fermi surface affected by the long-range magnetic order is larger in BaCo122, leaving less electronic states available for the superconducting state.

We should keep in mind that iron-based superconductors are very sensitive to scattering and even nonmagnetic disorder is pair breaking [66–68]. As is seen from Fig. 4, the residual resistivity of BaCo122 is substantially higher than that of BaK122 as was also studied in detail for BaCo122 [48] and BaK122 [69]. Dopant ions inevitably introduce substitutional disorder, particularly strong for substitution on Fe site, it is impossible to disentangle the effects of changing the Fermi levels from the pair-breaking scattering and it is quite possible that part of the observed asymmetry between hole- and electron-doped compounds is due to scattering.

We note that the nematic susceptibility is also weaker in the BaK122 family, as evidenced by the in-plane resistivity anisotropy behavior [39] and the softening of the shear modulus [47]. Therefore our findings suggest a close relationship between the electron-hole asymmetries of the normal state and superconducting properties. Despite displaying different magnitudes, however, the continuous increase of $\Delta\lambda(0.25T_c)$ with underdoping in both electron- and hole-doped samples contrasts with the case of isovalent doping, BaP122, in which a sharp peak in the low-temperature penetration depth is observed [70].

IV. CONCLUSIONS

In conclusion, our measurements of the London penetration depth in high quality single crystals of $Ba_{1-x}K_xFe_2As_2$ close to the optimal doping level $x = 0.34$ ($T_c = 39$ K) reveal a superconducting state with two full gaps $\Delta_1(0) = 6.5$ meV and $\Delta_2(0) = 3.3$ meV. Our measurements deep in the underdoped regime, for $x = 0.16$ ($T_c = 7$ K), demonstrate that the gap develops significant anisotropy without, however, developing nodes. Comparison with the electron-doped compositions $Ba(Fe_{1-x}Co_x)_2As_2$ reveals a strong asymmetry of the structure of the superconducting state, which is nodeless in hole-doped and nodal in electron-doped compounds. These observations suggest that the competition and the coexistence with magnetic/nematic order is responsible for the anisotropic structure of the superconducting gap in the underdoped regime, and that this competition is stronger in electron-doped rather than in hole-doped compounds.

ACKNOWLEDGMENTS

We thank A. Chubukov, P. Hirschfeld, S. Maiti, J. Schmalian, and L. Taillefer for useful discussions. The work at Ames was supported by the U.S. Department of Energy (DOE), Office of Science, Basic Energy Sciences, Materials Science and Engineering Division. The research was performed at the Ames Laboratory, which is operated for the U.S. DOE by Iowa State University under contract DE-AC02-07CH11358. Work in China was supported by the Ministry of Science and Technology of China, project 2011CBA00102. Work at Sherbrooke was supported by the Canadian Institute for Advanced Research and a Canada Research Chair, and it was funded by NSERC, FQRNT, and CFI.

[1] I. I. Mazin, Nature (London) **464**, 183 (2010).
[2] F. Wang and D.-H. Lee, Science **332**, 200 (2011).
[3] P. J. Hirschfeld, M. M. Korshunov, and I. I. Mazin, Rep. Prog. Phys. **74**, 124508 (2011); A. V. Chubukov, Annu. Rev. Cond. Mat. Phys. **3**, 57 (2012).
[4] R. T. Gordon C. Martin, H. Kim, N. Ni, M. A. Tanatar, J. Schmalian, I. I. Mazin, S. L. Bud'ko, P. C. Canfield, and R. Prozorov, Phys. Rev. B **79**, 100506 (2009).
[5] R. T. Gordon, N. Ni, C. Martin, M. A. Tanatar, M. D. Vannette, H. Kim, G. D. Samolyuk, J. Schmalian, S. Nandi, A. Kreyssig, A. I. Goldman, J. Q. Yan, S. L. Bud'ko, P. C. Canfield, and R. Prozorov, Phys. Rev. Lett. **102**, 127004 (2009).
[6] C. Martin, H. Kim, R. T. Gordon, N. Ni, V. G. Kogan, S. L. Bud'ko, P. C. Canfield, M. A. Tanatar, and R. Prozorov, Phys. Rev. B **81**, 060505 (2010).
[7] M. A. Tanatar, J.-Ph. Reid, H. Shakeripour, X. G. Luo, N. Doiron-Leyraud, N. Ni, S. L. Bud'ko, P. C. Canfield, R. Prozorov, and Louis Taillefer, Phys. Rev. Lett. **104**, 067002 (2010).
[8] J.-Ph. Reid, M. A. Tanatar, X. G. Luo, H. Shakeripour, N. Doiron-Leyraud, N. Ni, S. L. Bud'ko, P. C. Canfield, R. Prozorov, and Louis Taillefer, Phys. Rev. B **82**, 064501 (2010).
[9] K. Gofryk A. B. Vorontsov, I. Vekhter, A. S. Sefat, T. Imai, E. D. Bauer, J. D. Thompson, and F. Ronning, Phys. Rev. B **83**, 064513 (2011).
[10] S. L. Bud'ko, Ni Ni, and Paul C. Canfield, Phys. Rev. B **79**, 220516 (2009).
[11] F. Hardy, T. Wolf, R. A. Fisher, R. Eder, P. Schweiss, P. Adelmann, H. v. Löhneysen, and C. Meingast, Phys. Rev. B **81**, 060501 (2010).
[12] P. J. Hirschfeld and D. J. Scalapino, Physics **3**, 64 (2010).
[13] S. Maiti, M. M. Korshunov, T. A. Maier, P. J. Hirschfeld, and A. V. Chubukov, Phys. Rev. Lett **107**, 147002 (2011).
[14] K. Cho, M. A. Tanatar, N. Spyrison, H. Kim, Y. Song, Pengcheng Dai, C. L. Zhang, and R. Prozorov, Phys. Rev. B **86**, 020508 (2012).
[15] R. Prozorov, K. Cho, H. Kim, and M. A. Tanatar, J. Phys.: Conf. Ser. **449**, 012020 (2013).
[16] S. V. Borisenko, V. B. Zabolotnyy, D. V. Evtushinsky, T. K. Kim, I. V. Morozov, A. N. Yaresko, A. A. Kordyuk, G. Behr, A. Vasiliev, R. Follath, and B. Buchner, Phys. Rev. Lett. **105**, 067002 (2010).
[17] D. S. Inosov, J. S. White, D. V. Evtushinsky, I. V. Morozov, A. Cameron, U. Stockert, V. B. Zabolotnyy, T. K. Kim, A. A. Kordyuk, S. V. Borisenko, E. M. Forgan, R. Klingeler, J. T. Park, S. Wurmehl, A. N. Vasiliev, G. Behr, C. D. Dewhurst, and V. Hinkov, Phys. Rev. Lett. **104**, 187001 (2010).
[18] H. Kim, M. A. Tanatar, Yoo Jang Song, Yong Seung Kwon, and R. Prozorov, Phys. Rev. B **83**, 100502 (2011).
[19] M. A. Tanatar, J.-Ph. Reid, S. René de Cotret, N. Doiron-Leyraud, F. Laliberte, E. Hassinger, J. Chang, H. Kim, K. Cho, Yoo Jang Song, Yong Seung Kwon, R. Prozorov, and Louis Taillefer, Phys. Rev. B **84**, 054507 (2011).

[20] A. V. Chubukov, M. G. Vavilov, and A. B. Vorontsov, Phys. Rev. B **80**, 140515 (2009).

[21] R. Thomale, C. Platt, J. Hu, C. Honerkamp, and B. A. Bernevig, Phys. Rev. B **80**, 180505(R) (2009).

[22] K. Hashimoto, M. Yamashita, S. Kasahara, Y. Senshu, N. Nakata, S. Tonegawa, K. Ikada, A. Serafin, A. Carrington, T. Terashima, H. Ikeda, T. Shibauchi, and Y. Matsuda, Phys. Rev. B **81**, 220501 (2010).

[23] H. Ding, P. Richard, K. Nakayama, T. Sugawara, T. Arakane, Y. Sekiba, A. Takayama, S. Souma, T. Sato, T. Takahashi, Z. Wang, X. Dai, Z. Fang, G. F. Chen, J. L. Luo, and N. L. Wang, Europhys. Lett. **83**, 47001 (2008).

[24] K. Nakayama, T. Sato, P. Richard, Y.-M. Xu, T. Kawahara, K. Umezawa, T. Qian, M. Neupane, G. F. Chen, H. Ding, and T. Takahashi, Phys. Rev. B **83**, 020501 (2011).

[25] Z. Li, D. L. Sun, C. T. Lin, Y. H. Su, J. P. Hu, and Guo-qing Zheng, Phys. Rev. B **83**, 140506 (2011).

[26] C. Martin, R. T. Gordon, M. A. Tanatar, H. Kim, N. Ni, S. L. Bud'ko, P. C. Canfield, H. Luo, H. H. Wen, Z. Wang, A. B. Vorontsov, V. G. Kogan, and R. Prozorov, Phys. Rev. B **80**, 020501 (2009).

[27] K. Hashimoto, T. Shibauchi, S. Kasahara, K. Ikada, S. Tonegawa, T. Kato, R. Okazaki, C. J. van der Beek, M. Konczykowski, H. Takeya, K. Hirata, T. Terashima, and Y. Matsuda, Phys. Rev. Lett. **102**, 207001 (2009).

[28] X. G. Luo, M. A. Tanatar, J.-Ph. Reid, H. Shakeripour, N. Doiron-Leyraud, N. Ni, S. L. Bud'ko, P. C. Canfield, Huiqian Luo, Zhaosheng Wang, Hai-Hu Wen, R. Prozorov, and Louis Taillefer, Phys. Rev. B **80**, 140503 (2009).

[29] J. K. Dong, S. Y. Zhou, T. Y. Guan, H. Zhang, Y. F. Dai, X. Qiu, X. F. Wang, Y. He, X. H. Chen, and S. Y. Li, Phys. Rev. Lett. **104**, 087005 (2010).

[30] H. Fukazawa, T. Yamazaki, K. Kondo, Y. Kohori, N. Takeshita, P. M. Shirage, K. Kihou, K. Miyazawa, H. Kito, H. Eisaki, and A. Iyo, J. Phys. Soc. Jpn. **78**, 033704 (2009).

[31] K. Hashimoto, A. Serafin, S. Tonegawa, R. Katsumata, R. Okazaki, T. Saito, H. Fukazawa, Y. Kohori, K. Kihou, C. H. Lee, A. Iyo, H. Eisaki, H. Ikeda, Y. Matsuda, A. Carrington, and T. Shibauchi, Phys. Rev. B **82**, 014526 (2010).

[32] Z. Li, R. Zhou, Y. Liu, D. L. Sun, J. Yang, C. T. Lin, and G.-q. Zheng, Phys. Rev. B **86**, 180501 (2012).

[33] J.-Ph. Reid, M. A. Tanatar, A. Juneau-Fecteau, R. T. Gordon, S. René de Cotret, N. Doiron-Leyraud, T. Saito, H. Fukazawa, Y. Kohori, K. Kihou, C. H. Lee, A. Iyo, H. Eisaki, R. Prozorov, and Louis Taillefer, Phys. Rev. Lett. **109**, 087001 (2012).

[34] D. Watanabe, T. Yamashita, Y. Kawamoto, S. Kurata, Y. Mizukami, T. Ohta, S. Kasahara, M. Yamashita, T. Saito, H. Fukazawa, Y. Kohori, S. Ishida, K. Kihou, C. H. Lee, A. Iyo, H. Eisaki, A. B. Vorontsov, T. Shibauchi, and Y. Matsuda, Phys. Rev. B **89**, 115112 (2014).

[35] J.-Ph. Reid, A. Juneau-Fecteau, R. T. Gordon, S. Rene de Cotret, N. Doiron-Leyraud, X. G. Luo, H. Shakeripour, J. Chang, M. A. Tanatar, H. Kim, R. Prozorov, T. Saito, H. Fukazawa, Y. Kohori, K. Kihou, C. H. Lee, A. Iyo, H. Eisaki, B. Shen, H.-H. Wen, and Louis Taillefer, Supercond. Sci. Technol. **25**, 084013 (2012).

[36] R. M. Fernandes, D. K. Pratt, Wei Tian, J. Zarestky, A. Kreyssig, S. Nandi, Min Gyu Kim, A. Thaler, Ni Ni, P. C. Canfield, R. J. McQueeney, J. Schmalian, and A. I. Goldman, Phys. Rev. B **81**, 140501 (2010).

[37] S. Maiti, R. M. Fernandes, and A. V. Chubukov, Phys. Rev. B **85**, 144527 (2012).

[38] R. M. Fernandes, A. V. Chubukov, and J. Schmalian, Nat. Phys. **10**, 97 (2014).

[39] E. C. Blomberg, M. A. Tanatar, R. M. Fernandes, I. I. Mazin, B. Shen, H.-H. Wen, M. D. Johannes, J. Schmalian, and R. Prozorov, Nat. Commun. **4**, 1914 (2013).

[40] E. Hassinger, G. Gredat, F. Valade, S. Rene de Cotret, A. Juneau-Fecteau, J.-Ph. Reid, H. Kim, M. A. Tanatar, R. Prozorov, B. Shen, H.-H. Wen, N. Doiron-Leyraud, and Louis Taillefer, Phys. Rev. B **86**, 140502 (2012).

[41] S. Avci, J. M. Allred, O. Chmaissem, D. Y. Chung, S. Rosenkranz, J. A. Schlueter, H. Claus, A. Daoud-Aladine, D. D. Khalyavin, P. Manuel, A. Llobet, M. R. Suchomel, M. G. Kanatzidis, and R. Osborn, Phys. Rev. B **88**, 094510 (2013).

[42] V. G. Kogan, C. Martin, and R. Prozorov, Phys. Rev. B **80**, 014507 (2009).

[43] R. M. Fernandes and J. Schmalian, Phys. Rev. B **82**, 014520 (2010).

[44] D. Kuzmanovski and M. G. Vavilov, Supercond. Sci. Technol. **25**, 084001 (2012).

[45] A. Levchenko, M. G. Vavilov, M. Khodas, and A. V. Chubukov, Phys. Rev. Lett. **110**, 177003 (2013).

[46] D. Chowdhury, B. Swingle, E. Berg, and S. Sachdev, Phys. Rev. Lett. **111**, 157004 (2013).

[47] A. E. Bohmer, P. Burger, F. Hardy, T. Wolf, P. Schweiss, R. Fromknecht, M. Reinecker, W. Schranz, and C. Meingast, Phys. Rev. Lett. **112**, 047001 (2014).

[48] M. A. Tanatar, N. Ni, A. Thaler, S. L. Bud'ko, P. C. Canfield, and R. Prozorov, Phys. Rev. B **82**, 134528 (2010).

[49] M. A. Tanatar, W. E. Straszheim, H. Kim, J. Murphy, N. Spyrison, E. C. Blomberg, K. Cho, J.-P. Reid, B. Shen, L. Taillefer, H.-H. Wen, and R. Prozorov, Phys. Rev. B **89**, 144514 (2014).

[50] H. Q. Luo, Z. S. Wang, H. Yang, P. Cheng, X. Zhu, and H.-H. Wen, Supercond. Sci. Technol. **21**, 125014 (2008).

[51] C. T. van Degrift, Rev. Sci. Instrum. **46**, 599 (1975).

[52] R. Prozorov and R. W. Giannetta, Supercond. Sci. Technol. **19**, R41 (2006).

[53] R. Prozorov, R. W. Giannetta, A. Carrington, and F. M. Araujo-Moreira, Phys. Rev. B **62**, 115 (2000).

[54] R. Prozorov and V. G. Kogan, Rep. Prog. Phys. **74**, 124505 (2011).

[55] G. Li, W. Z. Hu, J. Dong, Z. Li, P. Zheng, G. F. Chen, J. L. Luo, and N. L. Wang, Phys. Rev. Lett. **101**, 107004 (2008).

[56] G. Mu, Huiqian Luo, Zhaosheng Wang, Lei Shan, Cong Ren, and Hai-Hu Wen, Phys. Rev. B **79**, 174501 (2009).

[57] S. Avci, O. Chmaissem, E. A. Goremychkin, S. Rosenkranz, J.-P. Castellan, D. Y. Chung, I. S. Todorov, J. A. Schlueter, H. Claus, M. G. Kanatzidis, A. Daoud-Aladine, D. Khalyavin, and R. Osborn, Phys. Rev. B **83**, 172503 (2011).

[58] M. Rotter, M. Tegel, and D. Johrendt, Phys. Rev. Lett. **101**, 107006 (2008).

[59] R. T. Gordon, H. Kim, N. Salovich, R. W. Giannetta, R. M. Fernandes, V. G. Kogan, T. Prozorov, S. L. Bud'ko, P. C. Canfield, M. A. Tanatar, and R. Prozorov, Phys. Rev. B **82**, 054507 (2010).

[60] E. G. Moon and S. Sachdev, Phys. Rev. B **85**, 184511 (2012).
[61] R. M. Fernandes, S. Maiti, P. Wölfle, and A. V. Chubukov, Phys. Rev. Lett. **111**, 057001 (2013).
[62] R. M. Fernandes and A. J. Millis, Phys. Rev. Lett. **111**, 127001 (2013).
[63] G. Livanas, A. Aperis, P. Kotetes, and G. Varelogiannis, arXiv:1208.2881.
[64] R. Thomale, C. Platt, W. Hanke, J. Hu, and B. A. Bernevig, Phys. Rev. Lett. **107**, 117001 (2011).
[65] F. Kretzschmar, B. Muschler, T. Bohm, A. Baum, R. Hackl, H.-H. Wen, V. Tsurkan, J. Deisenhofer, and A. Loidl, Phys. Rev. Lett. **110**, 187002 (2013).
[66] V. G. Kogan, Phys. Rev. B **80**, 214532 (2009).
[67] R. T. Gordon, H. Kim, M. A. Tanatar, R. Prozorov, and V. G. Kogan, Phys. Rev. B **81**, 180501 (2010).
[68] R. Prozorov, M. Konczykowski, M. A. Tanatar, A. Thaler, S. L. Bud'ko, P. C. Canfield, V. Mishra, and P. J. Hirschfeld, arXiv:1405.3255.
[69] Y. Liu, M. A. Tanatar, W. E. Straszheim, B. Jensen, K. W. Dennis, R. W. McCallum, V. G. Kogan, R. Prozorov, and T. A. Lograsso, Phys. Rev. B **89**, 134504 (2014).
[70] K. Hashimoto, K. Cho, T. Shibauchi, S. Kasahara, Y. Mizukami, R. Katsumata, Y. Tsuruhara, T. Terashima, H. Ikeda, M. A. Tanatar, H. Kitano, N. Salovich, R. W. Giannetta, P. Walmsley, A. Carrington, R. Prozorov, and Y. Matsuda, Science **336**, 1554 (2012).